

Electronic Supplementary Information

Enhanced cycling performance and electrochemical reversibility of novel sulfur-impregnated mesoporous hollow TiO₂ spheres cathode for advanced Li-S batteries

Jiaoyang Li,^{a,b} Bing Ding,^b Guiying Xu,^b Linrui Hou,^a Xiaogang Zhang^{b} and Changzhou Yuan^{a*}*

^a School of materials Science & Engineering, Anhui University of technology, Ma`anshan, 243002, P.R. China. E-mail:ayuan cz@163.com

^b College of Material Science and Engineering Nanjing University of Aeronautics and Astronautics, Nanjing, 210016, P.R. China. E-mail:azhang xg@163.com

Experimental Section

Carbon spheres were firstly synthesized *via* hydrothermal treatment of an aqueous glucose solution.¹ Then, 0.1 g of the carbon spheres were well dispersed in 40 ml of ethanol under ultrasonication for 2 h at room temperature, an appropriate amount of Ti(C₄H₉O)₄ was added and vigorously stirred for 60 min. Next, 70 ml of H₂O was added dropwise at a rate of 1 mL min⁻¹. Stirring was continued for another 12 h to allow complete hydrolyzation of the precursors. Finally, the precipitate was isolated by centrifugation and brown solid powders of C/Ti(OH)₄ were obtained after drying the sample at 60 °C in an oven.

The brown solid powders of C/Ti(OH)₄ were calcinated by applying specific procedures

reported recently.² Firstly, calcinations in a tube furnace under N₂ flow at 550 °C for 1 h (heating rate, 3 °C min⁻¹) was performed and then recalcination under air flow while keeping the same thermal conditions. As a result, hollow anatase TiO₂ spheres were obtained.

The as-prepared porous hollow TiO₂ spheres (30 mg) and sulfur (70 mg) were mixed together and placed in a crucible. Then mixture was then heated to 155 °C with a 0.2 °C min⁻¹ heating ramp, and kept at the temperature for 10 h to facilitate the sulfur diffusion into the hollow TiO₂ spheres. And no additional washing procedure was applied afterward. Finally, the S/hollow TiO₂ spheres were fabricated.

Materials characterization

The samples were examined by powder X-ray diffraction (XRD) (Max 18 XCE, Japan) using a Cu K α source ($\lambda = 0.154056$ nm) at a scanning speed of 3° min⁻¹ over a 2θ range of 10 - 80°. The morphologies and structures were observed with field-emission scanning electron microscopy (FESEM, JEOL-6300F, 15 kV) and transmission electron microscope (TEM, FEI TECNAI-20). N₂ adsorption/desorption was determined by Brunauer-Emmett-Teller (BET) measurement by using an ASAP-2010 surface area analyzer. The zeta potential of the as-synthesized TiO₂ was measured with a Malvern Instruments Zen 3600 nano-zs. X-ray photoelectron spectroscopy (XPS) measurements were performed on a VGESCALAB MKII X-ray photoelectron spectrometer with a Mg K α excitation source (1253.6 eV).

Electrochemical Measurements

The working electrode consisted of active material (S/hollow TiO₂ spheres or S), acetylene black, and polymer binder (polyvinylidene difluoride) (PVDF) at a weight ratio of 70 : 20 : 10 in N-methyl pyrrolidinone (NMP) solvent to form slurry. The resultant slurry was uniformly spread

onto pure aluminium foil using a doctor blade, and dried at 75 °C for 12 h. CR2016-type coin cells were fabricated by sandwiching a porous polypropylene separator between the working electrode and Li metal foil (Cyprus Foote Mineral, 99.98%, USA) in a high-purity Ar-filled glove box. The electrolyte used was 1 M lithium bis(trifluoromethanesulfonyl)imide (LiTFSI) and 0.1 M LiNO₃ in a mixed solvent of 1,3-dioxolane (DOL) and 1,2-dimethoxyethane (DME) with a volume ratio of 1 : 1. Galvanostatic discharge and charge cycling of the Li/S cells was conducted using an CT2001A tester (Wuhan, China) at several different rates between cut-off potentials of 1.5 and 3.0 V. Cyclic voltammograms (CV) and electrochemical impedance spectra (EIS) measurements were conducted with a CHI 600A electrochemical workstation at a scan rate of 0.2 mV s⁻¹. EIS measurements were conducted after the cell was fully charged to 3 V.

1 J. Ming, H. Cheng, Y. Yu, Y. Wu and F. Zhao, *J. Mater. Chem.*, 2011, **21**, 6654.

2 J. Ming, Y. Wu, L. Wang, Y. Yu and F. Zhao, *J. Mater. Chem*, 2011, **21**, 17776.

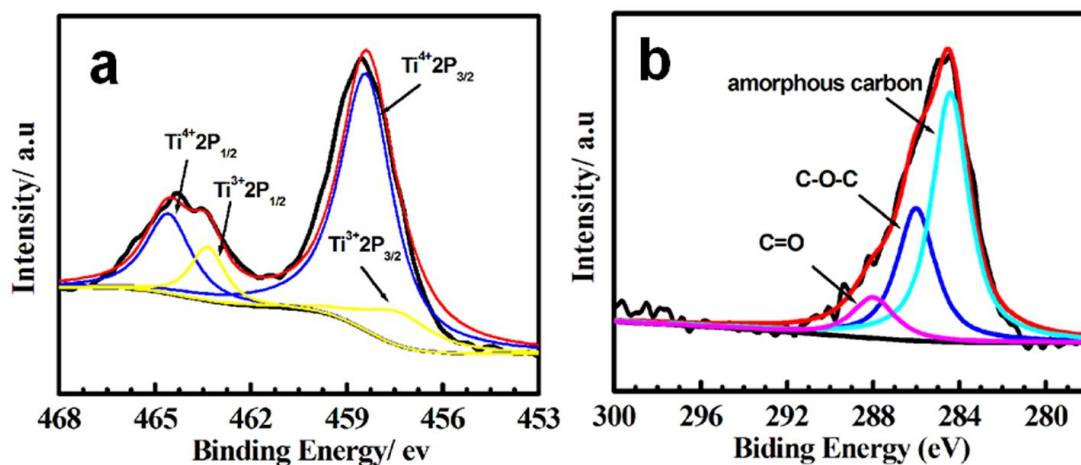


Fig. S1 High-resolution (a) Ti2p and (b) C1s XPS spectra for the as-prepared TiO₂ spheres.

X-ray photoelectron (XPS) measurements of the as-prepared TiO₂ spheres were performed, and the corresponding results are presented in Fig. S1. By using a Gaussian fitting method, the Ti 2p emission spectrum was best fitted with two spin-orbit doublets, characteristic of Ti⁴⁺ and Ti³⁺. Specifically, the doublet peaks at 458.4 and 464.6 eV corresponding to Ti 2p_{3/2} and Ti 2p_{1/2} respectively, demonstrate the existence of Ti⁴⁺. And another pair of smaller peaks sitting in 457.4 and 463.4 eV belongs to Ti 2p_{3/2} and Ti 2p_{1/2}, respectively, indicating the existence of Ti³⁺. Obviously, oxygen-deficient type titanium dioxide with low valence titanium ions was observed. In addition, less of 1 wt.% carbon still can be found in the as-prepared TiO₂ spheres. Fitting on carbon species, the C 1s core peaks also present three components. The first one, located at 284.4 eV, is assigned to amorphous carbon. And the two other C 1s core peaks at 286.1 and 288 eV are related to C-O-C and C=O bonds, respectively. Due to the two factors, the mesoporous hollow TiO₂ spheres with desirable electronic conductivity can be obtained as promising hosts for high-performance LSBs.

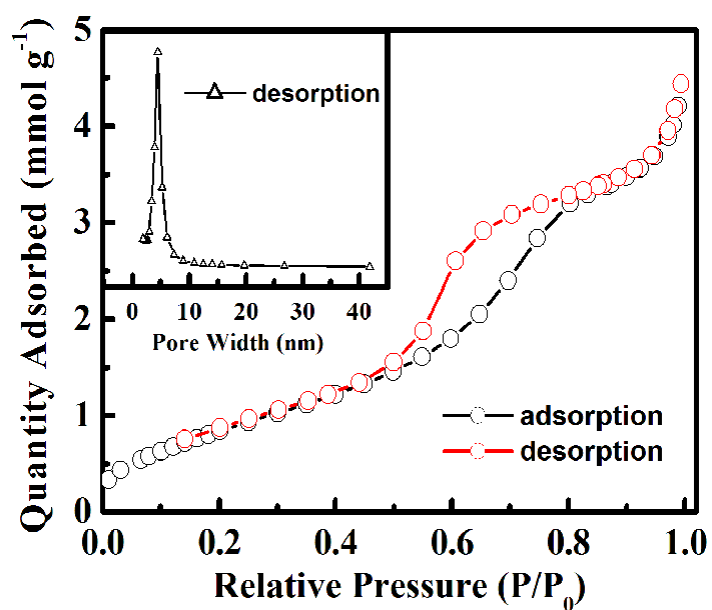


Fig. S2 N₂ adsorption-desorption isotherm curve and pore size distribution curve (the inset) of the hollow TiO₂ spheres.

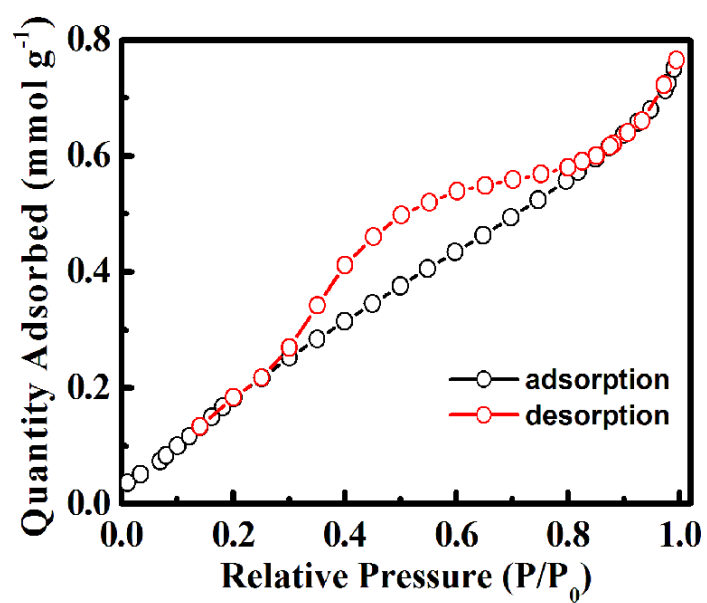


Fig. S3 N₂ adsorption-desorption isotherm curve of the S/HTSs.

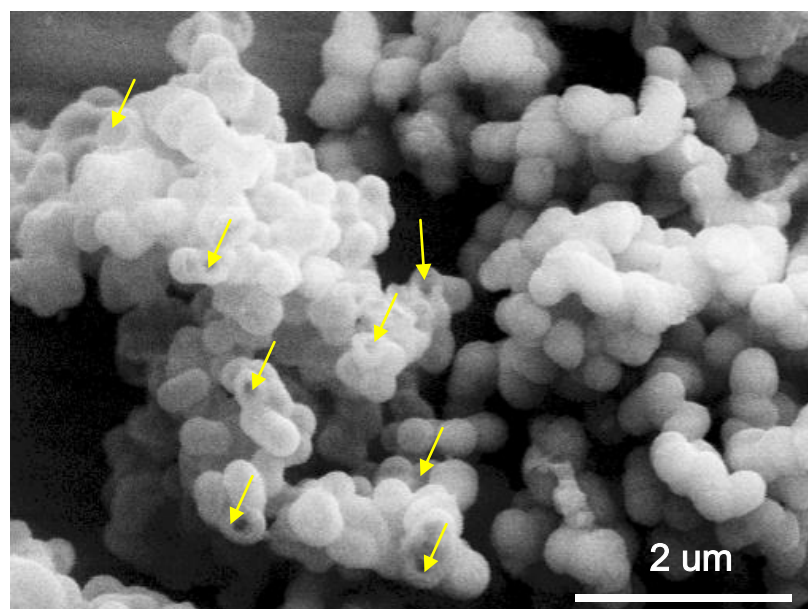


Fig. S4 FESEM image of the as-obtained hollow TiO₂ spheres

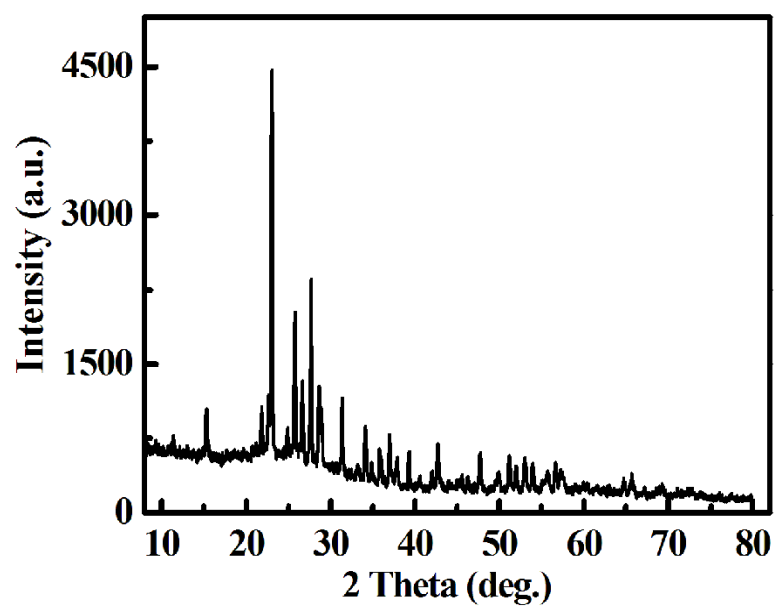


Fig. S5 X-ray diffraction pattern of the elemental S

Table S1. Comparison of the XRD diffraction peaks of the elemental S and the S/HTSs

	~23.1		~27.8	
	Height	FWHM ^(a)	Height	FWHM
Elemental S	4453	0.18	2327	0.17
S-TiO ₂	652	0.24	357	0.21

(a) full width at half maximum

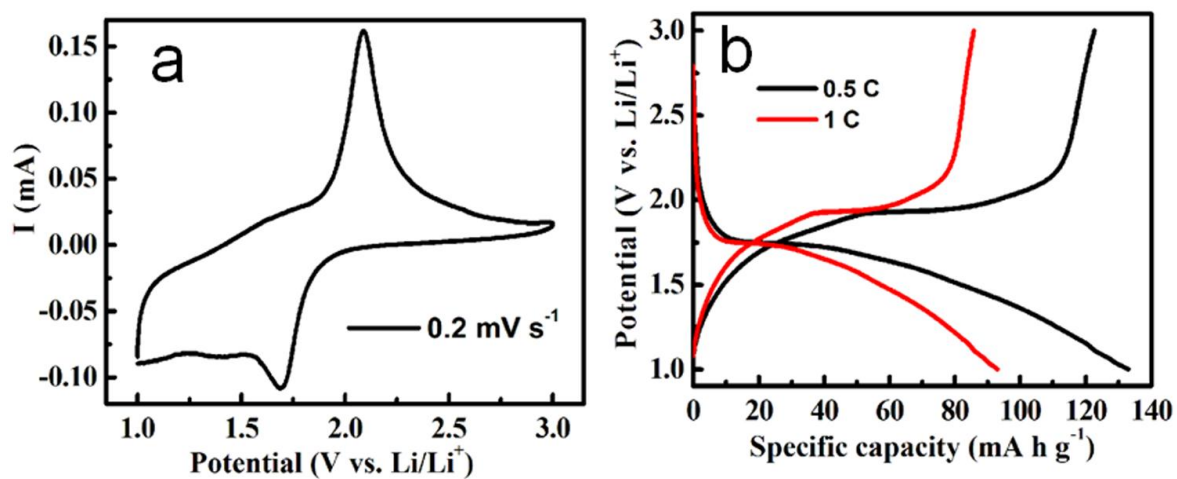


Fig. S6 (a) CV curve (0.2 mV s^{-1}) and (b) discharge/charge voltage profiles at various C rates (0.5 C and 1 C) of the mesoporous hollow TiO_2 spheres

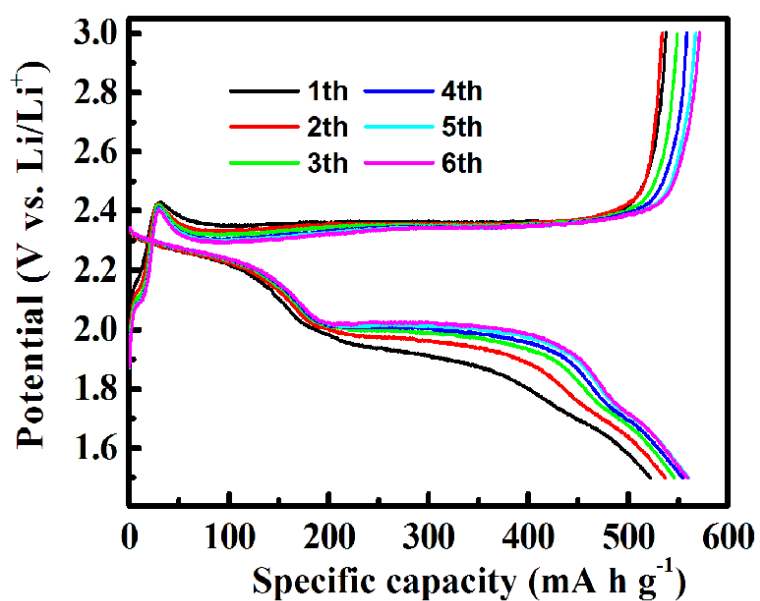


Fig. S7 First six discharge/charge potential vs. specific capacity under the potential window 3.0-1.5 V at 1 C rate

The good overlap of the discharge plateaus during the cycling test also suggested the good stability and reversibility of the electrode.

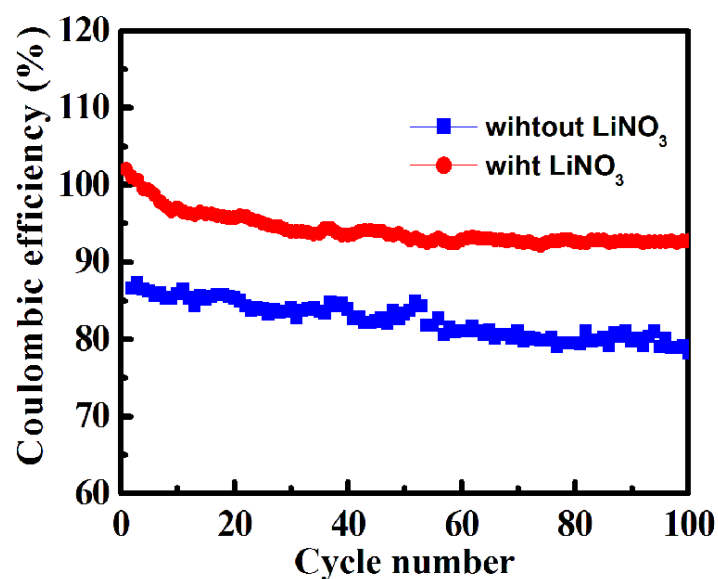


Fig. S8 Coulombic efficiency of the S/HTSs in different electrolytes as indicated at 1 C rate

As observed in Fig. S8, the electrolyte also plays a great role in enhancing the coulombic efficiency of the S/HTSs. Clearly, the coulombic efficiency reduces from 93% to 80% at 1C when LiNO₃ was not added. As is well known, LiNO₃ is as one of the critical components to form a protective SEI on lithium anode for lithium-sulfur system, which favors for improving the coulombic efficiency of lithium-sulfur cell as well.

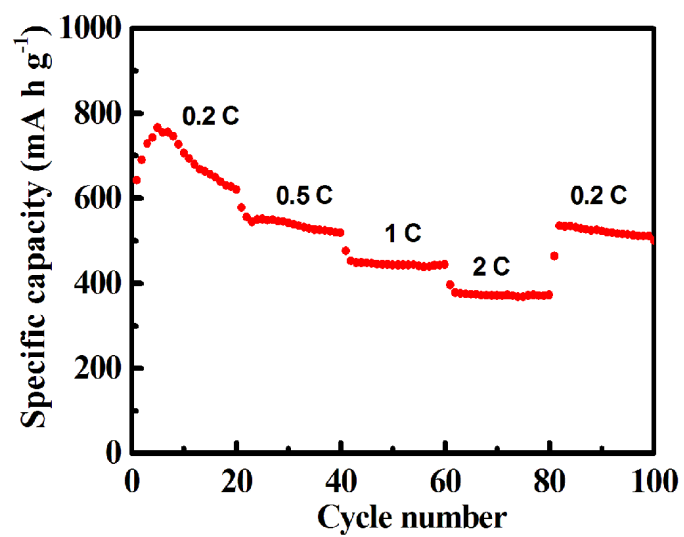


Fig. S9 Rate performance of the S/HTSs

Table S2 Electrochemical performance of the S/HTSs electrode in this study, compared with some other S composite cathodes with different S loadings reported in previous literatures

Electrodes with various S loadings	Capacity retention (red number) and coulombic efficiency (blue number) after cycling at certain C rates
S/HTSs (68 wt.%, this study)	71 % and 93% at 1 C after 100 cycle
S coated with polypyrrole nanolayers (63.3 wt.%, ref. 3)	73.4% and 90% at 0.2 C after 50 cycles
Core-shell structured S-polypyrrole composite (65 wt.%, ref. 4)	41.6% at 1 C after 50 cycles
S/polythiophene with a core/Shell Structure (71.9 wt.%, ref. 5)	74.2% and 92.2% at 100 mA/g after 80 cycles
Porous hollow carbon@S composites (70 wt.%, ref. 6)	91% and 94% at 0.5 C after 100 cycles
Highly ordered nanostructured carbon-S (70 wt.%, ref. 7)	83.3% at 0.1 C after 20 cycles
S impregnated disordered carbon nanotubes (40 wt.%, ref. 8)	72.9% and 96% at 0.25 C after 100 cycles
S/graphene nanocomposite (44.5 wt.%, ref. 9)	55.1% at 1 C after 100 cycles
Confining S in double-shelled hollow carbon spheres (64 wt.%, ref. 10)	67.6% at 0.1 C after 100 cycles
S/mesoporous carbon (50 wt.%, ref. 11)	60.4% at 0.1 C after 100 cycles
Graphene-S with PEG (70 wt.%, ref. 12)	70% at 0.2 C after 100 cycles
Sandwich-type functionalized graphene sheet-S (70 wt.%, ref. 13)	54% and 84.3% at 1 C after 100 cycles
S imbedded bimodal porous carbons (50 wt.%, ref. 14)	55.3% at 1 C after 100 cycles

3 Y. Fu and A. Manthiram, *J. Phys. Chem. C* 2012, **116**, 8910.

4 Y. Fu and A. Manthiram, *RSC Adv.* 2012, **2**, 5927.

5 F. Wu, J. Chen, R. Chen, S. Wu, L. Li, S. Chen and T. Zhao, *J. Phys. Chem. C* 2011, **115**, 6057.

6 N. Jayaprakash, J. Shen, S. S. Moganty, A. Corona and L. A. Archer, *Angew. Chem. Int. Ed.* 2011, **50**, 5904.

- 7 X. Ji, K. T. Lee and L. F. Nazar, *Nat. Mater.* 2009, **8**, 500.
- 8 J. Guo, Y. Xu and C. Wang, *Nano Lett.* 2011, **11**, 4288.
- 9 B. Wang, K. Li, D. Su, H. Ahn and G. Wang, *Chem. Asian J.* 2012, **7**, 1637.
- 10 C. F. Zhang, H. B. Wu, C. Z. Yuan, Z. P. Guo and X. W. Lou, *Angew. Chem. Int. Ed.* 2012, **51**, 9592.
- 11 X. Li, Y. Cao, W. Qi, L. V. Saraf, J. Xiao, Z. Nie, J. Mietek, J. G. Zhang, B. Schwenzer and J. Liu, *J. Mater. Chem.* 2011, **21**, 16603.
- 12 H. Wang, Y. Yang, Y. Liang, J. T. Robinson, Y. Li, A. Jackson, Y. Cui and H. Dai, *Nano Lett.* 2011, **11**, 2644.
- 13 Y. Cao, X. Li, I. A. Aksay, J. Lemmon, Z. Nie, Z. Yang and J. Liu, *Phys. Chem. Chem. Phys.* 2011, **13**, 7660.
- 14 G. He, X. Ji and L. Nazar, *Energy Environ. Sci.* 2011, **4**, 2878.

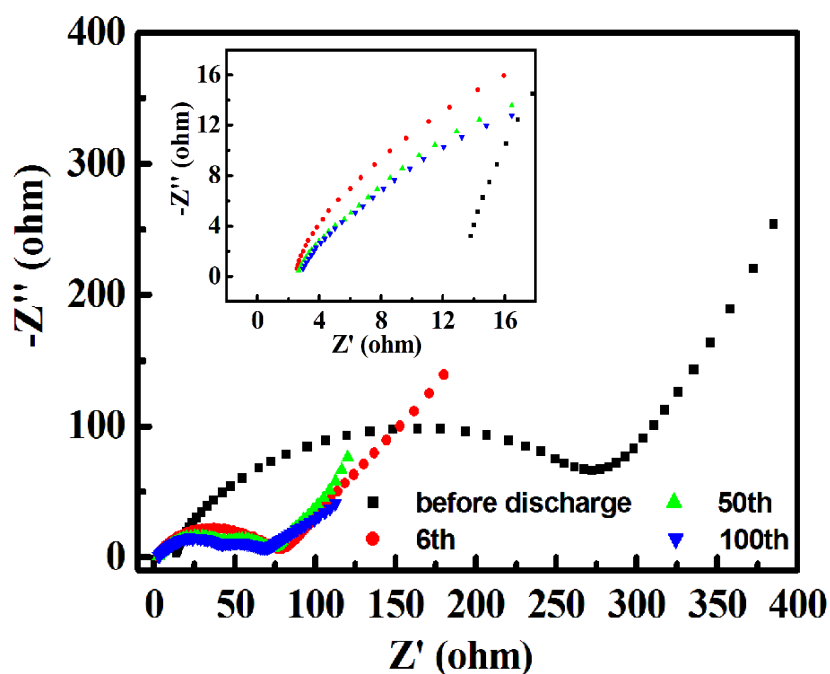


Fig. S10 Electrochemical impedance spectra at different depth of discharge of the S/HTSs electrode

These impedance data were gathered at ~ 3 V, the electrolyte is stable and should not form a solid electrolyte interphase (SEI). The electrical conductivity of the electroactive material itself under different cycles can be observed by the intercept of the electrode with the real impedance (Z') axis. And the high frequency semicircle reflects the charge transfer resistance (CRT) of the electroactive material under different cycles.